Electronic Supplementary Material (ESI) for Chemical Communications.

Supplementary Information

(8 Texts, 15 Figures, 2 Tables and 17 References)

Modulating the metal centers in MIL-101 for the piezoelectric catalytic synthesis of hydrogen peroxide

Yatai Li, Zhi Li, Xuecong Lin, Hao Lv and Mingshan Zhu*

Guangdong Key Laboratory of Environmental Pollution and Health, School of Environment, Jinan University, Guangzhou 511443, PR China

Correspondence and requests for materials should be addressed to M.Z. (zhumingshan@jnu.edu.cn).

Supplementary Texts

Text S1. Materials.

Chromium(III) nitrate nonahydrate ($Cr(NO_3)_3·9H_2O$), Ferric(III) nonahydrate ($Fe(NO_3)_3·9H_2O$), terephthalic acid (H_2BDC), N,N-Dimethylformamide (DMF) and hydrofluoric acid (HF) were obtained from Aladdin, Shanghai. Carbamazepine (CBZ), 5,5-dimethyl-1-pyrroline (DMPO), silver nitrate ($AgNO_3$), p-benzoquinone (p-BQ) and potassium hydrogen phthalate ($KHC_8H_4O_4$) were purchased from Aladdin Chemical Reagent Co., Ltd., China. tert-butanol (TBA), Potassium iodide (KI), ammonium molybdate ($(NH_4)_6Mo_7O_{24}·4H_2O$), Sodium sulfate (Na_2SO_4) and ethanol (EtOH) were purchased from Sinopharm Chemical Reagent Co., Ltd. All the reagents were of analytical grade and were used without further purification.

Text S2. Instruments.

The morphology was measured by Transmission Electron Microscope (TEM, JEOL 2010F) and field-emission scanning electron microscope (SEM, Ultra-55, Germany). The crystal structure of powder product was investigated via X-ray diffraction (XRD) D2 PHASER with Cu-Kα radiation with 2-theta degree from 10 to 70. Fourier transform infrared spectrophotometer (FT-IR) (IRTracer-100, Shimadzu, Japan) was used to explore organic structure. Thermo Scientific K-Alpha X-ray photoelectron spectroscopy system (Thermo Fisher Scientific, UK) was used to detect XPS signals. Piezoresponse force microscopy (PFM) with a scanning probe mode (Asylum Research, Nanoworld) was used to characterized the piezoelectric response of samples. 500 °C.

Text S3. Preparation of MIL-101(Cr) and MIL-101(Fe).

The MIL-101(Cr) and MIL-101(Fe) was synthesized by referring to the pervious literature.[1, 2] Typically, chromium(III) nitrate nonahydrate ($Cr(NO_3)_3·9H_2O$) (1.2 g) or Ferric(III) nonahydrate ($Fe(NO_3)_3·9H_2O$) (1.2 g), terephthalic acid (H_2BDC) (500 mg), hydrofluoric acid (HF) (0.09 mL) were mixed with 15 mL H_2O in a Teflon-lined stainless steel autoclave, and then it was heated to 220 ^oC for 8 h. After cooling down to the

room temperature, the mixture was centrifuged and washed with N,N-Dimethylformamide (DMF) and deionized water. Finally, the green solids were dried under vacuum at 80 ^{o}C for 10 h.

Text S4. Piezoelectric catalytic H_2O_2 production.

2 mg of catalyst was added to 10 mL of pure water containing ethanol (10 vol%). The catalyst was dispersed by ultrasonication for 10 min, and air was bubbled through the solution for 10 min. The reactor was kept at 25 ± 0.5°C with cooling circulating water and was subjected to ultrasonication by an ultrasonic (Us) cleaner (40 kHz, 100 W, Jielimei, Kunshan, China). The concentration of H_2O_2 was measured by the KI colorimetric method.[3] One milliliter of freshly prepared KI reagent A (0.4 M KI, 0.05 M NaOH, 1.6×10^{-4} M $(NH_4)_6Mo_7O_{24}\cdot 4H_2O$) and 1 ml of reagent B (0.1 M $KHC_8H_4O_4$) were mixed with 1 mL of the above samples. The absorbance of the above mixture was measured at 350 nm by a UV–Vis spectrophotometer (JASCO V-770, Japan). To study the effects of gases, different gases, including N_2, O_2 and air, were bubbled through the solution for 15 min to conduct subsequent experiments.

Text S5. Electrochemical measurement.

All electrochemical measurements are made through an electrochemical workstation (CHI 760E), including transient piezoelectric current curve, electrochemical impedance spectroscopy (EIS), Mott–Schottky measurement, Linear sweep voltammetry (LSV). Three-electrode system was prepared with sample modified GCE, Pt wire and Saturated Calomel Electrode (SCE) as the working, counter and reference electrodes, respectively. The basic voltage of transient piezoelectric current curve was set to 0.38 V. Electrochemical impedance spectroscopy was performed at an initial potential of 0.38 V, a range of 0.1-10^4 Hz and amplitude of 5 mV. LSV has a voltage sweep range from 1 to -1V, at a scan rate of 0.1V/s and a sensitivity of 10^{-5} A/V. The supporting electrolyte is 0.5M Na_2SO_4.

Text S6. Mott–Schottky measurement.

Tests of Mott-Schottky plots are investigated to obtain carrier density of MIL-101(Cr) and MIL-101(Fe). The positive straight line slope under constant frequency of 1000 Hz manifests that MIL-101(Cr) and MIL-101(Fe) are n-type semiconductor.

Additionally, the flat band potential (V_{fb}) can be estimated by extrapolating the line to $1/C^2 = 0$ with the following equation:

$$\frac{1}{C^2} = \frac{2}{A^2 e \varepsilon_r \varepsilon_0 N_d}\left(V - V_{fb} - \frac{kT}{e}\right)$$

where C is the specific capacity, A is the effective surface area, ε_r and ε_0 are dielectric constants of the catalyst and vacuum, respectively, e is elementary charge and N_d is the carrier concentration of the catalyst, V is the applied potential while V_{fb} is the flat band potential, k is the Boltzmann constant and T represents absolute temperature.[4] The carrier concentration (N_d) was calculated from the slopes (S) of the Mott–Schottky plots:

$$N_d = \frac{2}{A^2 e \varepsilon_r \varepsilon_0 S}$$

The ratio of S of the two MOFs is inversely proportional to the ratio of N_d, Since A, ε_r, ε_0 and e of them are all approximately equal. Accordingly, the ratio of carrier concentration values of MIL-101(Cr) and MIL-101(Fe) estimated from the slope is 2.66.[5]

Text S7. Piezoelectric catalytic degradation experiments.

Briefly, 2 mg of the as-prepared catalyst was dispersed in pure water (10 mL) then sonicated for 10 min. The target pollutant of CBZ was subsequently added into the above suspension. Then, the reactor was placed in ultrasonic cleaner. After filtration, the concentration of CBZ was determined by using high-performance liquid chromatography (HPLC, Agilent).

Text S8. EPR measurement.

10 μL DMPO was added 90 μL of 1mg/L catalyst of DMSO solution. Afterwards, the above solution was sonicated for 0, 1, 2, 3 and 5 min, respectively. The solution of 10 μL was absorbed by capillary tube, sealed and measured in EPR.

Supplementary Figures

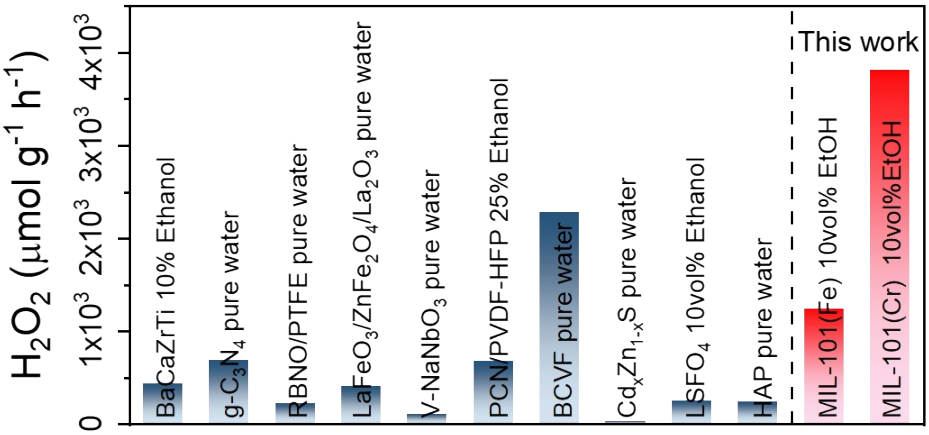

Figure S1: H_2O_2 production rates for MIL-101(Cr) in this work compared with reported piezoelectric catalytic work. Corresponding reports are shown in **Table S1**.

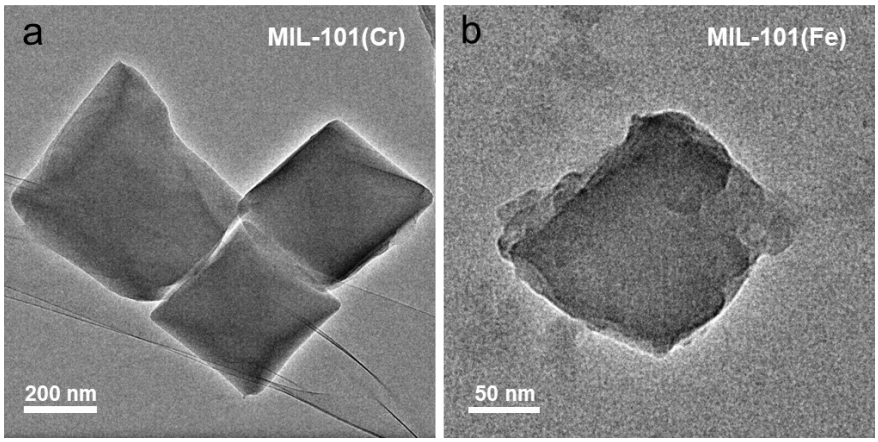

Figure S2: TEM images of (**a**) MIL-101(Cr)and MIL-101(Fe) (**b**).

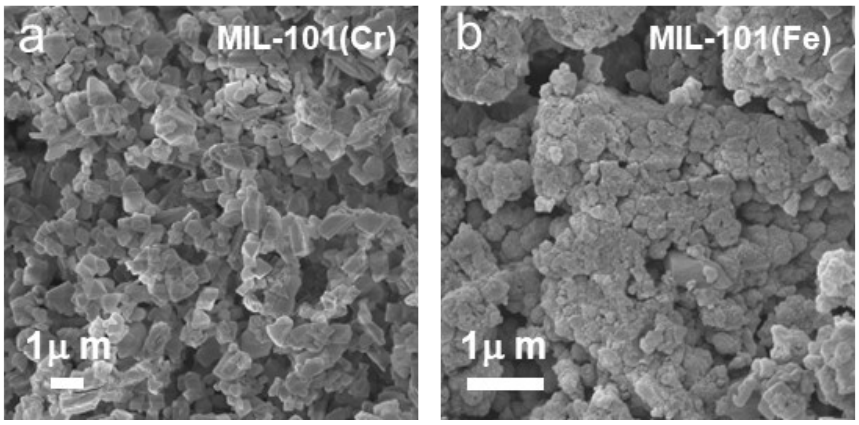

Figure S3: TEM images of MIL-101(Cr) (**a**) and MIL-101(Fe) (**b**).

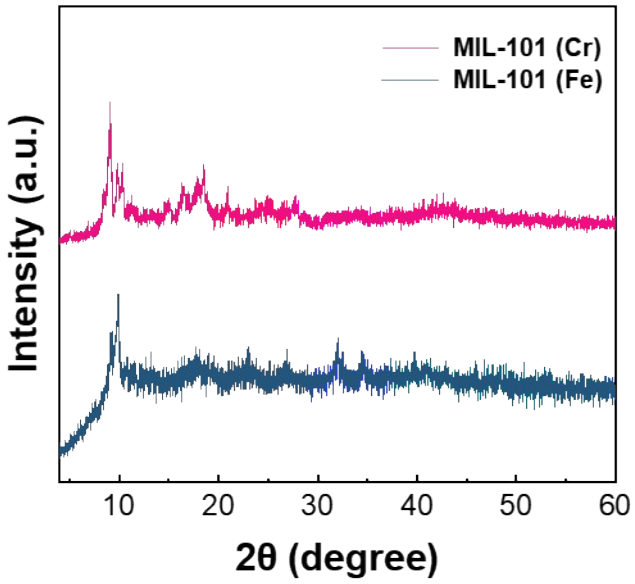

Figure S4: XRD patterns of MIL-101(Fe) and MIL-101(Cr).

The XRD patterns of MIL-101(Fe) and MIL-101(Cr) materials are presented in **Fig. S4**. As seen from the figure, MIL-101 (Fe) has obvious diffraction peaks at 2θ values of 8. 8°, 9.4°, 18.9°, and 23.7°, while MIL-101(Cr) displays sharp peaks at 2θ = 8.7°, 9.4°, 10.2°, 16.7°, 18.5°, 28.5°, and these results are similar with previous reports.[2, 6]

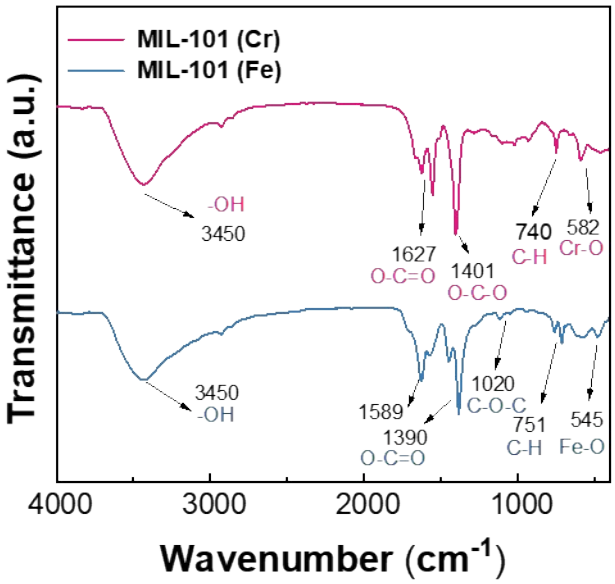

Figure S5: FT-IR spectra of MIL-101(Fe) and MIL-101(Cr).

The chemical bond features of MIL-101(Fe) and MIL-101(Cr) were explored by Fourier transform infrared spectroscopy (FT-IR) (**Fig. S5**). Both MIL-101 (Fe) and MIL-101(Cr) show sharp peaks at 1000-1700 cm^{-1}, corresponding to the typical vibration bands from the O-C-O group and the symmetric and asymmetric vibrations of O–C=O in carboxyl groups, and the peaks at 740-750 cm^{-1} are attributed to the C-H vibration of aromatic rings. Notably, MIL-101(Fe) displays an intense peak at 545 cm^{-1}, assigning to the Fe–O bond, while MIL-101(Cr) show a sharp peak at 582 cm^{-1}, revealing the existence of Cr–O bond.[6, 7] Both samples exhibit a hydroxyl peak at 3450 cm^{-1} due to the presence of water.

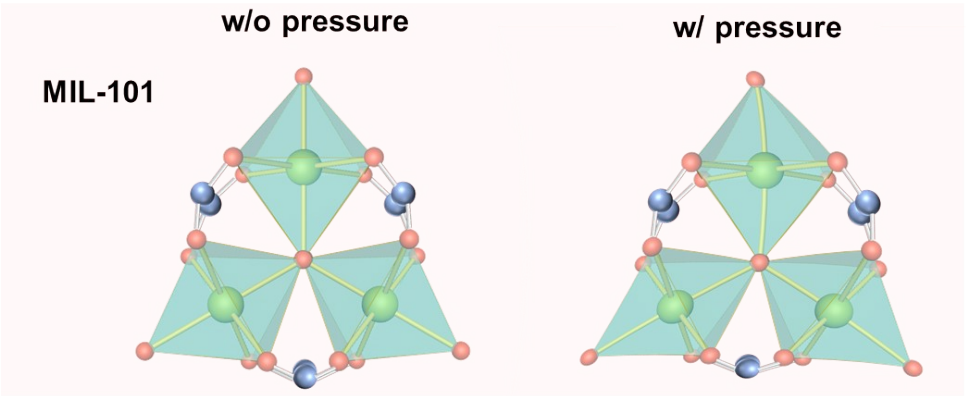

Figure S6: Molecular model change of MIL-101 with and without pressure.

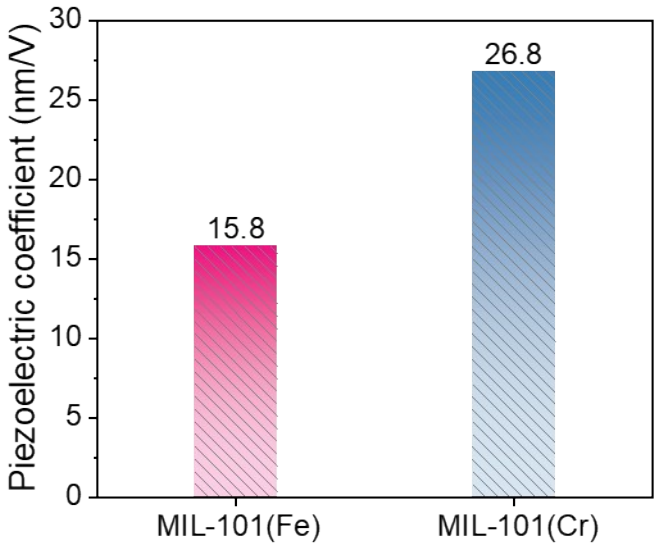

Figure S7: The piezoelectric coefficient of MIL-101(Fe) and MIL-101(Cr).

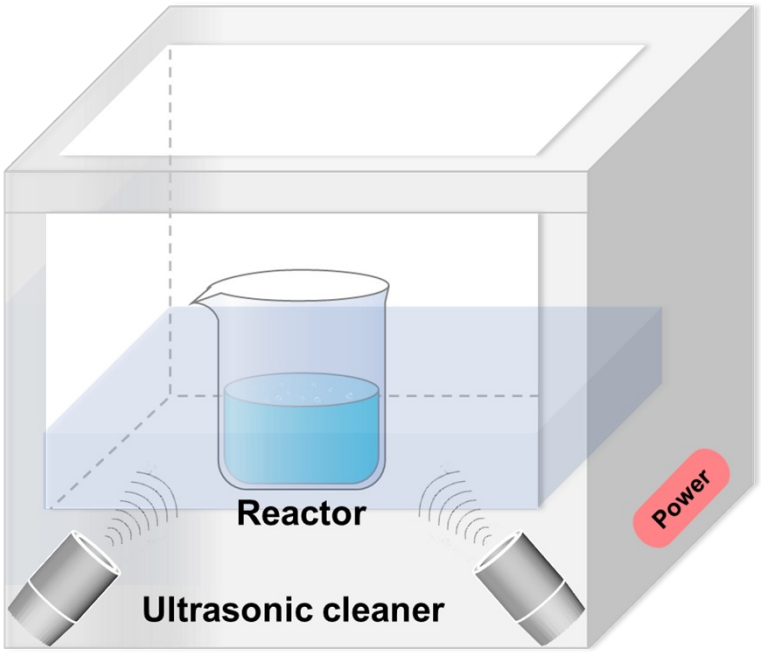

Figure S8: System for piezoelectric catalytic synthesis of H_2O_2.

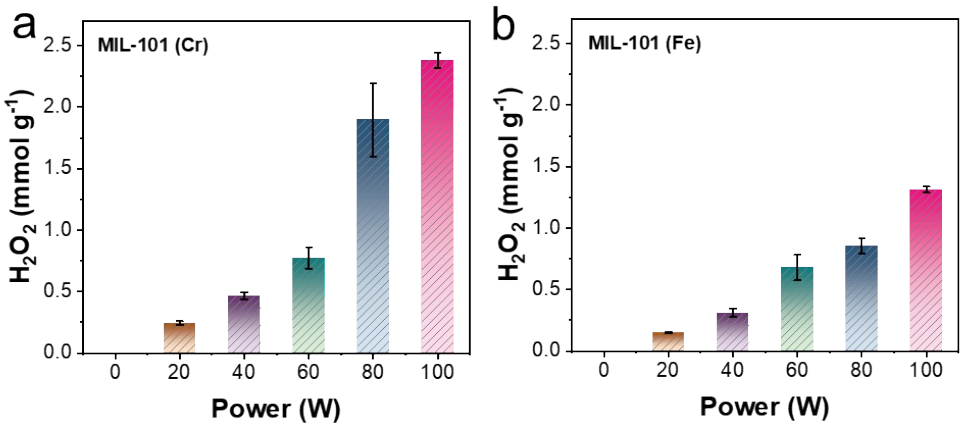

Figure S9: H_2O_2 production of MIL-101 (Cr) and MIL-101 (Fe) at different ultrasonic power.

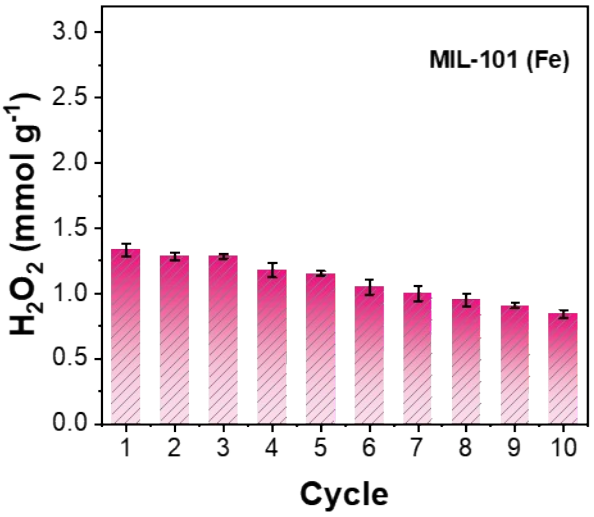

Figure S10: Stability test of MIL-101(Fe) for 10 cycles.

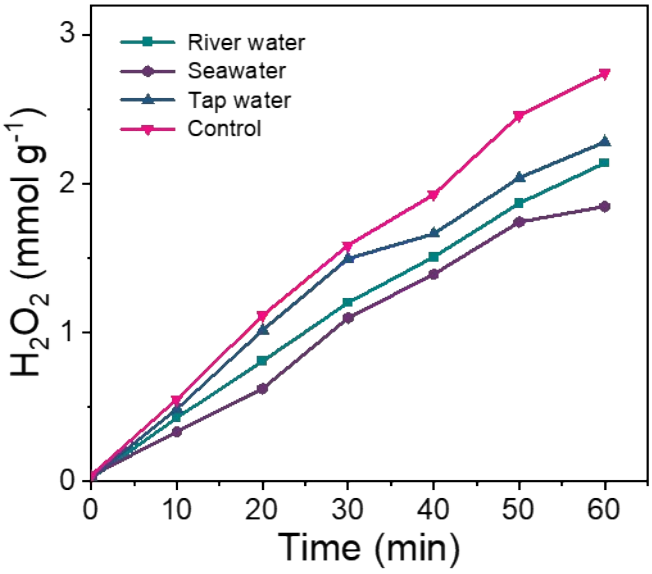

Figure S11: H_2O_2 production of MIL-101 (Cr) with real water samples.

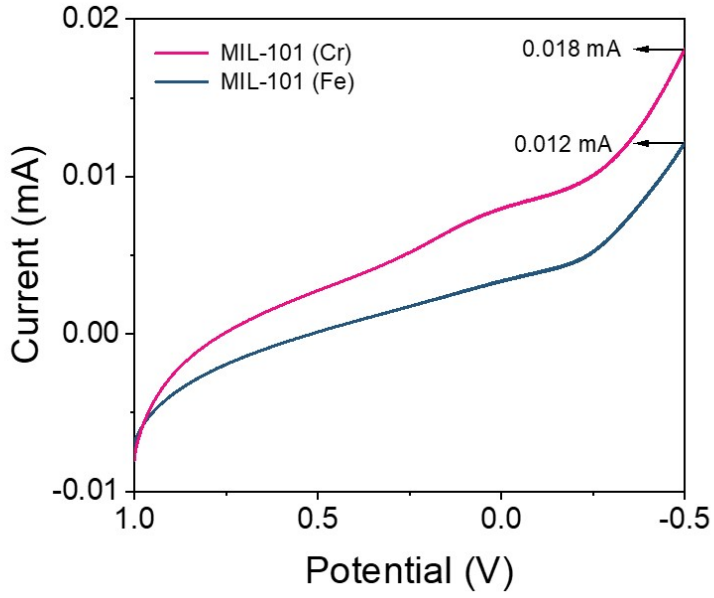

Figure S12: LSVs of MIL-101(Cr) and MIL-101(Fe).

The current reflects the ability of charge transport and it can be seen that MIL-101(Cr) has a current of 0.018 mA at -0.5 V, while MIL-101(Fe) displays that of 0.012 mA.

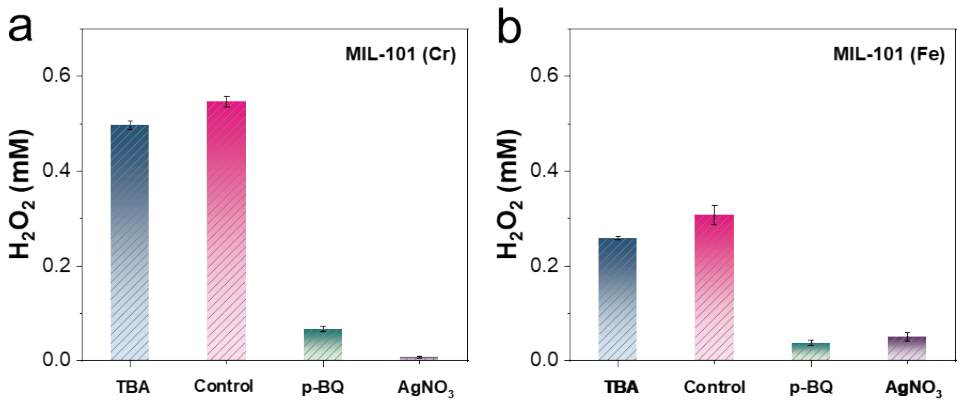

Figure S13: Scavenger tests of MIL-101(Cr) (**a**) and MIL-101(Fe) (**b**) in piezoelectric H_2O_2 production with Us at 60 min (TBA for ·OH, p-BQ for $\cdot O_2^-$ and $AgNO_3$ for e^-, *C*=5 mM).

Compared with control, the H_2O_2 yield decreased intensely with the addition of $AgNO_3$ or p-BQ, demonstrating that the electron and $\cdot O_2^-$ was the reactant and intermediate of H_2O_2 generation; while the yield of H_2O_2 decreased only slightly after the addition of TBA to burst the ·OH. These results are fully consistent with the reaction mechanism of ORR, which could be proposed by following Equation:

$$O_2 + H^+ + e^- \rightarrow \cdot O_2^- \quad (1)$$

$$\cdot O_2^- + 2H^+ + e^- \rightarrow H_2O_2 \quad (2)$$

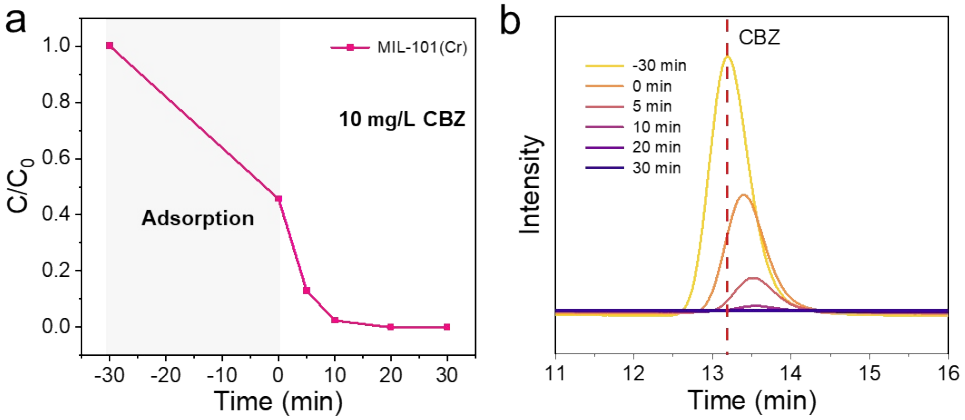

Figure S14: CBZ degradation with MIL-101(Cr) (**a**) and the corresponding HPLC spectra (**b**).

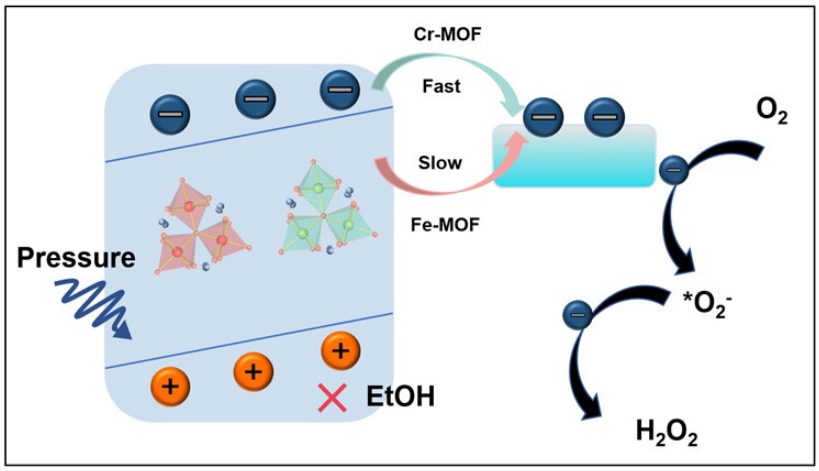

Figure S15: Mechanism of piezoelectric catalytic H_2O_2 generation by MIL-101(Cr) and MIL-101(Fe).

Supplementary Tables

Table S1. H_2O_2 production rates for MIL-101(Cr) in this work compared with representative recently reported work.

Catalysts	Condition	sacrificial agent	H_2O_2 ($\mu mol\ g^{-1}\ h^{-1}$)	Reference
BaCaZrTi	Us	10 vol% EtOH	433	[8]
g-C_3N_4	Us		680	[9]
RBNO/PTFE	Us		219.23	[10]
$LaFeO_3/ZnFe_2O_4/La_2O_3$	Us		403	[11]
V-$NaNbO_3$	Us		102.6	[12]
PCN/PVDF-HFP	Us	25 vol% EtOH	668.56	[13]
BCVF	Us		2271	[14]
$Cd_xZn_{1-x}S$	Us		21.9	[15]
$LSFO_4$	Us	10 vol% EtOH	247	[16]
HAP	Us		234	[17]
MIL-101(Fe)	Us	10 vol% EtOH	1310	This work
MIL-101(Cr)	Us	10 vol% EtOH	2760	This work

Table S2. R_{ct} values for two samples.

Catalysts	**R_{ct} (Ω)**
MIL-101(Fe)	5.58×10^5
MIL-101(Cr)	2.34×10^5

Supplementary References

1. G.-Y. Jeong, A. K. Singh, M.-G. Kim, K.-W. Gyak, U. Ryu, K. M. Choi and D.-P. Kim, *Nat. Commun.*, 2018, **9**, 3968.
2. Z. Li, H. Zhang, Q. Zha, C. Zhai, W. Li, L. Zeng and M. Zhu, *Microchim. Acta*, 2020, **187**, 526.
3. C. Hu, H. Huang, F. Chen, Y. Zhang, H. Yu and T. Ma, *Adv. Funct. Mater.*, 2020, **30**, 1908168.
4. J. Ke, J. Liu, H. Sun, H. Zhang, X. Duan, P. Liang, X. Li, M. O. Tade, S. Liu and S. Wang, *Appl. Catal. B: Environ.*, 2017, **200**, 47-55.
5. A. A. Dubale, W.-N. Su, A. G. Tamirat, C.-J. Pan, B. A. Aragaw, H.-M. Chen, C.-H. Chen and B.-J. Hwang, *J. Mater. Chem. A*, 2014, **2**, 18383-18397.
6. Z. Liu, W. He, Q. Zhang, H. Shapour and M. F. Bakhtari, *ACS Omega*, 2021, **6**, 4597-4608.
7. F. Zhang, T. Niu, F. Wu, L. Wu, G. Wang and J. Li, *Electrochim. Acta*, 2021, **392**, 139028.
8. K. Wang, M. Zhang, D. Li, L. Liu, Z. Shao, X. Li, H. Arandiyan and S. Liu, *Nano Energy*, 2022, **98**, 107251.
9. K. Wang, D. Shao, L. Zhang, Y. Zhou, H. Wang and W. Wang, *J. Mater. Chem. A*, 2019, **7**, 20383-20389.
10. Y. Ma, B. Wang, Y. Zhong, Z. Gao, H. Song, Y. Zeng, X. Wang, F. Huang, M.-R. Li and M. Wang, *Chem. Eng. J.*, 2022, **446**, 136958.
11. L. Zhang, K. Wang, Y. Jia, L. Fang, C. Han, J. Li, Z. Shao, X. Li, J. Qiu and S. Liu, *Adv. Funct. Mater.*, 2022, **32**, 2205121.
12. Y. Li, L. Li, F. Liu, B. Wang, F. Gao, C. Liu, J. Fang, F. Huang, Z. Lin and M. Wang, *Nano Res.*, 2022, **15**, 7986-7993.
13. Z. Chen, J. Zhuang, C. Liu, M. Chai, S. Zhang, K. Teng, T. Cao, Y. Zhang, Y. Hu and L. Zhao, *ChemElectroChem*, 2022, **9**, e202200124.
14. K. T. Wong, C. E. Choong, I. W. Nah, S.-H. Kim, B.-H. Jeon, Y. Yoon, E. H. Choi and M. Jang, *Appl. Catal. B: Environ.*, 2022, **315**, 121581.
15. S. Lin, Q. Wang, H. Huang and Y. Zhang, *Small*, 2022, **18**, 2200914.
16. L. Fang, K. Wang, C. Han, X. Li, P. Li, J. Qiu and S. Liu, *Chem. Eng. J.*, 2023, 141866.
17. G. Yin, C. Fu, F. Zhang, T. Wu, S. Hao, C. Wang and Q. Song, *J. Alloys Compd.*, 2023, **937**, 168382.